e-ISSN: 2807-6257

Open Access Indonesian Journal of Medical Reviews

[OAIJMR]

https://hmpublisher.com/index.php/oaijmr

When the Lung Deceives: Spindle Cell Carcinoma Manifesting as an Aggressive Posterior Mediastinal Mass – A Multimodal Imaging Case Report

Anggita Putri Kantilaras[1*]

[1]Department of Radiology, Faculty of Medicine and Health Sciences, Universitas Muhammadiyah Yogyakarta, Bantul, Indonesia

ARTICLE INFO

Keywords:
Lung cancer
Mediastinal mass
Non-small cell lung carcinoma
Posterior mediastinum
Spindle cell carcinoma

***Corresponding author:**
Anggita Putri Kantilaras

E-mail address:
anggita.p.kantilaras@mail.com

The author has reviewed and approved the final version of the manuscript.

https://doi.org/10.37275/oaijmr.v5i4.764

A B S T R A C T

Spindle cell carcinoma (SpCC) of the lung is a rare and aggressive subtype of non-small cell lung carcinoma (NSCLC), characterized by a significant component of spindle-shaped tumor cells. Its radiological presentation is highly variable, typically appearing as peripheral or central lung masses. Presentation as a primary mediastinal mass is exceedingly uncommon, posing a considerable diagnostic challenge. A 47-year-old woman presented with a 4-month history of progressive lower limb weakness. Initial chest radiography revealed a left-sided mediastinal-appearing mass. Subsequent contrast-enhanced computed tomography (CT) of the thorax characterized a large, lobulated soft tissue mass in the left posterior mediastinum, measuring 5.25 × 4.74 cm. The mass exhibited homogeneous isodensity with peripheral calcification, caused 0.5 cm compression of the descending aorta, and showed erosion of the 4th thoracic vertebra with contrast enhancement. Fine needle aspiration (FNA) cytology, guided by CT, demonstrated atypical, polymorphic spindle-shaped cells within a fibroangiomatous stroma, consistent with spindle cell carcinoma. In conclusion, this case highlights an unusual presentation of pulmonary SpCC mimicking a posterior mediastinal tumor with aggressive features, including vascular compression and vertebral erosion. Despite its mediastinal appearance, subtle radiological signs such as the acute angle with the lung parenchyma, the epicenter of the mass, and the irregular tumor-lung interface suggested a pulmonary origin. This report underscores the importance of meticulous radiological evaluation and cytopathological correlation in diagnosing rare lung cancer variants that can masquerade as primary mediastinal neoplasms.

1. Introduction

Lung cancer remains the leading cause of cancer-related mortality worldwide, with non-small cell lung carcinoma (NSCLC) accounting for the vast majority of cases. Within the heterogeneous group of NSCLCs, sarcomatoid carcinomas represent a rare and particularly aggressive collection of poorly differentiated tumors, constituting only 0.1% to 0.4% of all lung malignancies. Spindle cell carcinoma (SpCC), a distinct subtype of sarcomatoid carcinoma, is defined by the World Health Organization (WHO) as a poorly differentiated NSCLC containing a component of malignant spindle cells, often admixed with giant cells or other NSCLC subtypes. These tumors are characterized by their aggressive clinical behavior, propensity for early metastasis, and generally poor prognosis compared to other NSCLC variants. The median survival for patients with sarcomatoid carcinomas is often reported to be less than one year.[1,2]

Histopathologically, SpCC is composed predominantly or exclusively of spindle-shaped cells that may exhibit features of epithelial differentiation on immunohistochemistry or ultrastructural analysis, though these can sometimes be difficult to discern, leading to diagnostic overlap with true sarcomas. The diagnostic criteria stipulate that at least 10% of the tumor must comprise these spindle cells. These cells are typically arranged in fascicles or storiform patterns and can be associated with a variable inflammatory

infiltrate. The aggressive nature of SpCC is often reflected in its high mitotic rate, cellular atypia, and areas of necrosis.[3,4]

Radiologically, SpCC of the lung most commonly presents as a large, solitary peripheral mass, often greater than 5 cm in diameter, with a predilection for the upper lobes. These masses may exhibit well-defined or infiltrative margins, and cavitation can occur. Central, endobronchial lesions are less common but have been described. Invasion of adjacent structures, such as the chest wall or mediastinum, is frequently observed at the time of diagnosis, reflecting the tumor's aggressive biology. However, presentation as a mass that appears to arise primarily from the mediastinum is exceedingly rare, occurring in less than 5% of SpCC cases. Such presentations create significant diagnostic dilemmas, as the differential diagnosis for a posterior mediastinal mass is broad, encompassing neurogenic tumors, lymphomas, esophageal neoplasms, cysts, and metastases from other primary sites.[5,6]

Differentiating a peripheral lung tumor with mediastinal involvement from a true primary mediastinal tumor invading the lung can be challenging, particularly when the mass is large and extensively abuts or encases mediastinal structures. Several radiological signs have been proposed to aid in this distinction, including the "acute angle sign" (where a lung-based mass forms an acute angle with the mediastinum), the "epicenter concept" (determining whether the bulk of the tumor lies within the lung or mediastinum), and the characteristics of the tumor-lung interface (irregular or spiculated margins suggesting a lung primary).[7,8]

The patient in this report presented with neurological symptoms secondary to suspected spinal involvement, further complicating the initial diagnostic picture, as spinal canal invasion is often associated with primary posterior mediastinal neoplasms, particularly neurogenic tumors. However, it can also occur with aggressive lung cancers.

This case report describes an unusual and challenging instance of pulmonary SpCC in a 47-year-old female, which radiologically mimicked an aggressive primary posterior mediastinal mass with vertebral erosion and aortic compression. The novelty of this case lies in its exceptionally rare presentation, which underscores the diagnostic difficulties encountered when SpCC deviates from its typical radiological patterns, particularly in its manifestation as an apparent mediastinal lesion with significant local invasion.[9,10] This report aims to meticulously document the multimodal imaging findings, correlate them with the cytopathological diagnosis, and review the pertinent literature to highlight the radiological clues that can aid in differentiating such deceptive lung malignancies from true mediastinal tumors, thereby emphasizing the crucial role of a comprehensive diagnostic approach in guiding appropriate patient management for this aggressive and uncommon cancer. Furthermore, this study seeks to contribute to the limited body of literature on SpCC presenting as a primary mediastinal mass, providing insights that may assist clinicians and radiologists in navigating similar diagnostically challenging scenarios.

2. Case Presentation

A 47-year-old Indonesian woman was referred to the Pulmonary Clinic at PKU Muhammadiyah Gamping Hospital on January 2nd, 2025, with a distressing and progressively worsening chief complaint: weakness in both lower limbs that had insidiously begun approximately four months prior. The onset was subtle; she initially noticed a slight unsteadiness when rising from a seated position and a novel sense of fatigue in her legs after short walks. Over the ensuing weeks, this evolved into a more pronounced bilateral symmetrical weakness, significantly more marked in the proximal muscle groups of her thighs than in her calves or feet. She described difficulty climbing stairs, needing to use her arms to pull herself up, and a growing challenge in standing up from a low chair or the floor. Ambulation became increasingly laborious, her gait less steady, compelling her to reduce her daily activities

substantially. She explicitly denied any precipitating trauma. While she initially denied sensory symptoms, on more detailed questioning during the neurological assessment, she admitted to a vague, poorly localized sensation of "heaviness" and intermittent, mild paresthesias described as "pins and needles" in both lower extremities, though no clear dermatomal distribution or distinct sensory level was initially reported. There were no initial complaints of radicular pain. Importantly, she maintained normal bowel and bladder control, with no episodes of incontinence or urinary retention. Her appetite was preserved, and she reported no significant weight loss, fever, night sweats, persistent cough, dyspnea at rest or on exertion, chest pain, or hemoptysis. A comprehensive review of other systems was largely unremarkable.

Her past medical history was notable for a diagnosis of breast cancer three years prior, in 2022. This was an infiltrative ductal carcinoma of the left breast, clinical stage T2N1M0, Grade III. Hormone receptor status at the time was estrogen receptor (ER) positive, Progesterone Receptor (PR) positive, and human epidermal growth factor receptor 2 (HER2) negative. She had undergone a left modified radical mastectomy followed by six cycles of adjuvant chemotherapy with a regimen of doxorubicin and cyclophosphamide, followed by paclitaxel (AC-T). Subsequently, she received adjuvant radiotherapy to the chest wall and regional lymphatics and was on adjuvant endocrine therapy with tamoxifen. Her surveillance for breast cancer, including annual mammography of the right breast and regular clinical follow-ups, had shown no evidence of local recurrence or distant metastasis prior to this new presentation. She had no other significant chronic medical conditions, no known allergies, and was a lifetime non-smoker with no history of significant alcohol consumption or illicit drug use. Her occupational history was as a homemaker, with no known hazardous environmental exposures. Her family history was negative for lung cancer but included a maternal aunt with postmenopausal breast cancer.

On physical examination at the current presentation (January 2nd, 2025), she appeared comfortable at rest but visibly anxious. Her vital signs were: blood pressure 139/89 mmHg, heart rate 101 beats per minute and regular, respiratory rate 22 breaths per minute and unlabored, and temperature 36.8°C. Her weight was 46 kg, and her height was 159 cm, yielding a body mass index of 18.2 kg/m². The neurological examination was particularly pertinent. Cranial nerves II-XII were intact. Motor examination of the upper extremities revealed normal tone, bulk, and 5/5 power in all muscle groups bilaterally. In the lower extremities, however, there was increased muscle tone (spasticity) bilaterally. Muscle bulk appeared preserved. Power assessment using the Medical Research Council (MRC) scale showed: hip flexion 3/5 bilaterally, hip extension 3/5 bilaterally, knee extension 3+/5 bilaterally, knee flexion 3+/5 bilaterally, ankle dorsiflexion 4/5 bilaterally, and ankle plantarflexion 4/5 bilaterally. Deep tendon reflexes were markedly brisk in the lower extremities (3+ for patellar and Achilles reflexes bilaterally) and 2+ in the upper extremities. Bilateral Babinski signs (upgoing plantar reflexes) were elicited. Hoffmann's sign was absent. Sustained clonus was not elicited at the ankles. Sensory examination revealed symmetrically diminished light touch and pinprick sensation from approximately the T8-T10 dermatomal level downwards, a feature that became more apparent during this detailed examination. Vibration sense, tested with a 128 Hz tuning fork, was diminished at the ankles and knees compared to the upper limbs. Proprioception was intact in the toes. Cerebellar examination, including finger-nose-finger testing and heel-to-shin testing, was normal, as was the assessment for dysdiadochokinesia. Her gait, when attempted with support, was spastic and unsteady. The respiratory examination revealed symmetrical chest expansion. Tactile fremitus was normal. Percussion note was resonant over all lung fields. On auscultation, breath sounds were vesicular and clear bilaterally, with no added sounds such as wheezes, crackles, or rubs. Cardiovascular examination

revealed a regular tachycardia (101 bpm) with normal S1 and S2 heart sounds and no murmurs, rubs, or gallops. Peripheral pulses were palpable and symmetrical. Abdominal examination was unremarkable, with no organomegaly or palpable masses. There was no palpable cervical, supraclavicular, or axillary lymphadenopathy. The previous left mastectomy scar was well-healed, and there were no signs of local breast cancer recurrence on the chest wall.

Given the subacute onset of progressive myelopathy in a patient with a history of malignancy, urgent investigation was initiated. A plain chest radiograph (posteroanterior and lateral views) was performed on January 4th, 2025. This study demonstrated a relatively well-demarcated, ovoid opacity measuring approximately 5 cm in its largest dimension, located in the left mid-lung zone, superimposed over the cardiac silhouette and posterior thoracic structures. On the lateral view, the mass was clearly situated posteriorly, projecting over the thoracic vertebral bodies estimated to be at the T5 to T7 levels (Figure 1). The margins of this opacity appeared macroscopically smooth but subtly irregular upon closer inspection, particularly at its interface with the visible lung parenchyma. Notably, the mass formed an acute, sharp angle with the posterior mediastinal contour, rather than the obtuse, gently sloping angle typically seen with purely mediastinal masses. No definite spiculation was identified, nor was there evidence of cavitation, pleural effusion, or pneumothorax. The visible hilar structures and pulmonary vasculature appeared unremarkable. The cardiomediastinal silhouette, apart from the described mass, was within normal limits.

To better delineate this posterior thoracic mass, characterize its extent, and assess for vertebral or neural involvement given the patient's neurological symptoms, a contrast-enhanced computed tomography (CT) scan of the thorax was performed on January 8th, 2025. The CT examination was conducted using helical acquisition with intravenous administration of 100 mL of non-ionic iodinated contrast medium. Images were reconstructed in axial, sagittal, and coronal planes with soft tissue, lung, and bone algorithms. The CT scan confirmed the presence of a large, solid, lobulated soft tissue mass primarily located in the left posterior paraspinal region, consistent with the posterior mediastinal compartment but with features suggesting aggressive behavior and possible pulmonary origin. The mass measured 5.25 cm in transverse diameter by 4.74 cm in anteroposterior diameter on axial images (Figure 2A), with an estimated craniocaudal extent of approximately 6.0 cm, spanning from the level of the VTh4 to VTh7 vertebral bodies. On pre-contrast images, the mass appeared relatively homogeneous with an isodensity to skeletal muscle, with average attenuation values in the range of 40-50 Hounsfield Units (HU). Following contrast administration, the tumor demonstrated avid and relatively uniform enhancement, with post-contrast HU values increasing to 80-100 HU, indicative of significant vascularity. Foci of amorphous, peripheral calcification were noted along the posterior and lateral aspects of the mass (Figure 2A, 2B). The relationship of the mass to adjacent structures was critical. Medially, the tumor was intimately associated with the thoracic spine. There was unequivocal evidence of osseous destruction involving the left aspect of the VTh4 vertebral body, including the pedicle and transverse process (Figure 2B). The destructive process appeared to extend into the left neural foramen at the T4-T5 level, potentially compromising the exiting nerve root and abutting the anther-lateral aspect of the thecal sac. There was no clear evidence of intradural extension, but epidural tumor extension was highly suspected. Anteriorly, the mass exerted a distinct mass effect upon the descending thoracic aorta, causing an estimated 0.5 cm of indentation and slight anterior displacement of this major vessel (Figure 2D). The fat plane between the mass and the aorta was partially effaced. Laterally and anterolaterally, the mass interfaced with the medial aspect of the left lower lobe. While the tumor bulk was paravertebral, its epicenter appeared to be located at

the junction of the lung parenchyma and the mediastinum, with the mass bulging into both compartments. The interface with the lung parenchyma was predominantly irregular and somewhat ill-defined in areas, forming acute angles with the visceral pleura of the lung (Figure 2C). There was no associated consolidation, significant atelectasis, or pleural effusion. The visualized portions of the remaining lung fields were clear. No other suspicious mediastinal, hilar, or axillary lymphadenopathy was identified separate from the primary mass itself.

In light of the aggressive radiological features—vertebral erosion and aortic compression—and the urgent need for a definitive diagnosis to guide therapy, particularly for the patient's myelopathy, a CT-guided fine needle aspiration (FNA) of the left thoracic mass was performed on the same day, January 8th, 2025. Under CT fluoroscopic guidance, using a posterior paraspinal approach with the patient in the prone position, a 20-gauge Chiba needle was advanced into the enhancing portion of the mass, avoiding major vessels and the calcified periphery. Multiple aspirations were performed, yielding adequate material for cytological examination. The procedure was well-tolerated by the patient, with no immediate complications.

The FNA smears were processed with Papanicolaou and May-Grünwald-Giemsa stains. Microscopic examination revealed highly cellular aspirates (Figure 3A, 3B). The predominant cell type consisted of overtly malignant cells, largely spindle-shaped, with some pleomorphism (variation in size and shape). These cells were often arranged in loose, disorganized fascicles and cohesive clusters, as well as singly dispersed. Individual tumor cells exhibited elongated, hyperchromatic to vesicular nuclei with irregular nuclear contours, coarsely clumped chromatin, and generally inconspicuous or small nucleoli. The cytoplasm was scant to moderate in amount, pale, and ill-defined. Nuclear atypia was marked, and mitotic figures, including some atypical forms, were readily identified. The background stroma was notably fibroangiomatous, characterized by delicate, branching capillary-sized blood vessels intertwined with fine collagenous fibers, within which the spindle tumor cells were embedded. No definite glandular, squamous, or neuroendocrine differentiation was apparent on the cytological preparations. Scattered lymphocytes and neutrophils were also present in the background. Based on these cytomorphological features—the presence of a predominant population of atypical, malignant spindle cells with high mitotic activity—a diagnosis highly suggestive of spindle cell carcinoma (a subtype of sarcomatoid carcinoma) was rendered. The pathologist recommended that, if a larger biopsy specimen became available, immunohistochemical stains for cytokeratins (such as AE1/AE3, CAM5.2), vimentin, TTF-1, p63/p40, and S100 protein would be valuable to confirm the epithelial origin (and sarcomatoid differentiation) and to exclude other spindle cell neoplasms such as primary sarcoma or metastatic melanoma.

The patient's case, with its complex clinical presentation and concerning radiological and cytopathological findings, was promptly discussed at the multidisciplinary tumor board meeting. Participants included radiologists, pulmonologists, medical oncologists, radiation oncologists, thoracic surgeons, and pathologists. The differential diagnoses considered included a primary aggressive lung cancer (such as SpCC or another NSCLC with sarcomatoid features) with mediastinal and vertebral invasion, a primary posterior mediastinal sarcoma, a malignant peripheral nerve sheath tumor (given the posterior mediastinal location and foraminal involvement), or, less likely given the cytology, a metastatic lesion from her previous breast cancer (perhaps a metaplastic carcinoma variant, though these are rare). The consensus, strongly guided by the FNA cytology, favored a primary pulmonary spindle cell carcinoma presenting with this unusual pattern of growth and aggressive local invasion. Given the locally advanced nature of the tumor with extensive vertebral erosion causing significant neurological compromise and the compression of the descending aorta, the tumor was

deemed unresectable at initial presentation. The immediate priorities were to address the spinal cord compression and to establish a comprehensive treatment plan. The board recommended urgent palliative radiotherapy to the involved thoracic spine (VTh4 region) to alleviate pain and attempt to halt or reverse neurological progression. This was to be followed by systemic therapy, the nature of which would depend on further molecular testing of the tumor tissue (if sufficient material was available from the FNA cell block or if a core biopsy was subsequently obtained) for targetable mutations (such as MET exon 14 skipping, PD-L1 expression).

Figure 1. Pulmonary tumor at the level of the 5th-7th thoracic vertebrae, oval-shaped, forming an acute angle appearance.

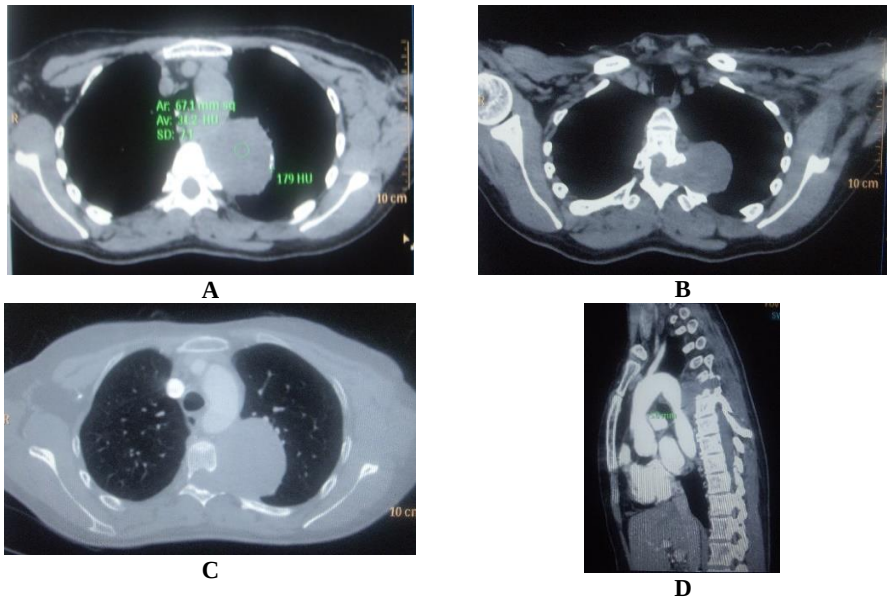

Figure 2. Contrast-enhanced CT imaging reveals aggressive features of the posterior mediastinal mass. (A) Axial soft tissue window demonstrating the lobulated, enhancing tumor with peripheral calcification. (B) Axial bone window highlighting destructive erosion of the 4th thoracic vertebra. (C) Axial lung window showing the tumor's irregular interface with the left lung parenchyma. (D) Sagittal reconstruction illustrating compression of the descending aorta by the mass.

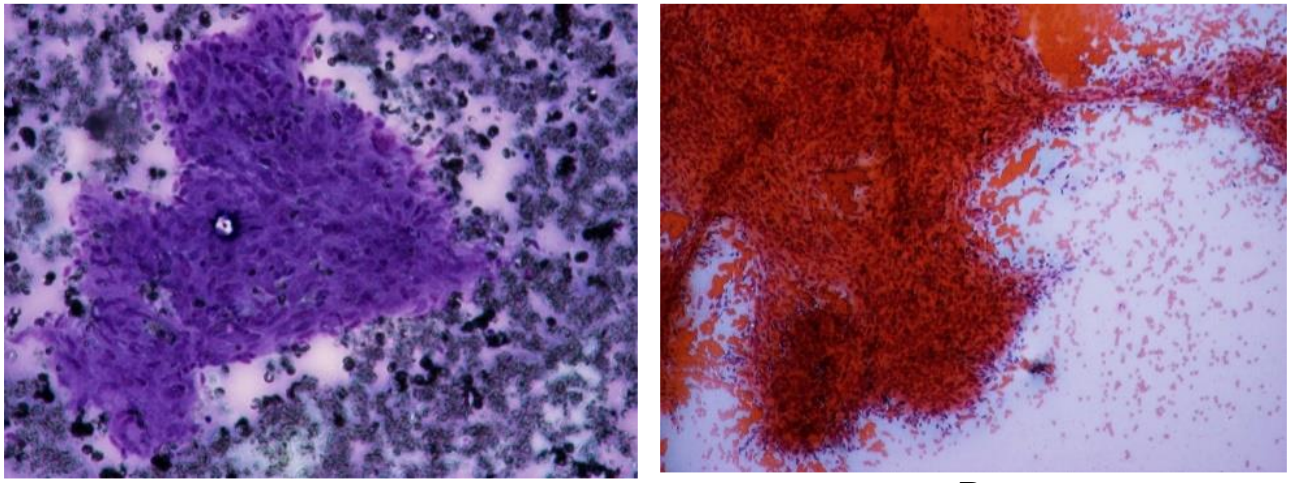

Figure 3. Cytopathological evidence of spindle cell carcinoma from CT-guided fine needle aspiration. (A) Cellular smear showing clusters of atypical, polymorphic spindle cells with hyperchromatic nuclei (Hematoxylin and Eosin stain). (B) Aspirate displaying malignant spindle cells embedded within a fibroangiomatous stroma (Papanicolaou stain or similar).

3. Discussion

The confluence of clinical, radiological, and cytopathological findings in this 47-year-old woman presents a compelling, albeit diagnostically intricate, narrative of pulmonary spindle cell carcinoma (SpCC) that deviated significantly from its more common presentations. This tumor's manifestation as an aggressive mass, appearing to arise from the posterior mediastinum and causing severe neurological compromise through vertebral destruction, alongside vascular compression, underscores the deceptive potential and inherent biological aggression of this rare NSCLC subtype. Spindle cell carcinoma belongs to the family of pulmonary sarcomatoid carcinomas, a group defined by the WHO as poorly differentiated non-small cell lung carcinomas that contain a component of spindle and/or giant cells, or are composed entirely of such cells. The very term "sarcomatoid" hints at the core enigma: these are carcinomas of epithelial origin that have undergone a profound morphological and behavioral transformation, acquiring features reminiscent of sarcomas (mesenchymal malignancies). This transformation is widely believed to be driven by the process of epithelial-mesenchymal transition (EMT).[11,12]

EMT is a fundamental biological process crucial during embryonic development, wound healing, and tissue fibrosis, but it is also pathologically hijacked by cancer cells to promote invasion and metastasis. During EMT, epithelial cells progressively lose their characteristic features, such as apical-basal polarity, tight cell-to-cell junctions (mediated by E-cadherin), and expression of epithelial markers like cytokeratins. Concurrently, they acquire mesenchymal traits, including a spindle-shaped morphology, enhanced motility, invasiveness, resistance to apoptosis, and expression of mesenchymal markers like vimentin, N-cadherin, fibronectin, and transcription factors such as Snail, Slug, Twist, and ZEB1/2. In SpCC, this transition is not merely a morphological curiosity; it underpins the tumor's aggressive clinical behavior. The spindle cells observed in this patient's FNA—elongated, pleomorphic, with hyperchromatic nuclei and indistinct cytoplasm, arranged in fascicles—are the cytological embodiment of this EMT process. The "polymorphism" and "atypia" reflect the uncontrolled

proliferation and genetic instability inherent in high-grade malignancies.[13,14]

The genetic landscape of sarcomatoid carcinomas, including SpCC, is complex and heterogeneous but offers clues to their aggressive nature. Mutations in TP53 are very common, occurring in up to 70-80% of cases, contributing to genomic instability and loss of apoptotic control. Alterations in KRAS, EGFR, BRAF, and PIK3CA have also been reported, though often at frequencies different from conventional NSCLC adenocarcinomas or squamous cell carcinomas. Notably, MET exon 14 skipping mutations are found in a significant subset (up to 20-30%) of pulmonary sarcomatoid carcinomas and are associated with sensitivity to MET inhibitors. Other alterations may involve genes like KEAP1, STK11/LKB1, and NF1. This genetic turmoil likely fuels the EMT process and sustains the aggressive phenotype. For instance, signaling pathways like TGF-β, Wnt/β-catenin, and Notch, often dysregulated in cancer, are potent inducers of EMT. Growth factors secreted by tumor cells or stromal cells can activate these pathways, leading to the transcriptional upregulation of EMT-inducing transcription factors.[15,16]

The fibroangiomatous stroma noted in the FNA is another critical component of the tumor microenvironment in SpCC. This is not a passive scaffold but an active participant in tumor progression. The "angiomatous" part refers to the rich network of blood vessels, a result of tumor-induced angiogenesis, often driven by factors like Vascular Endothelial Growth Factor (VEGF) secreted by the tumor cells. These neovessels are frequently abnormal—tortuous, leaky, and poorly organized—but they supply the tumor with nutrients and oxygen, facilitating its rapid growth, and also serve as conduits for hematogenous metastasis. The "fibro" component refers to the desmoplastic reaction, involving proliferation of cancer-associated fibroblasts (CAFs) and deposition of extracellular matrix proteins. CAFs can be recruited from resident fibroblasts or transdifferentiated from other cell types (including epithelial cells via EMT). They actively communicate with cancer cells, secreting growth factors, cytokines, and matrix-remodeling enzymes that promote tumor proliferation, invasion, and chemoresistance.[17,18]

Immunohistochemistry is indispensable for confirming the diagnosis of SpCC. The hallmark is the (often variable or focal) expression of cytokeratins (including AE1/AE3, CAM5.2, CK7) within the spindle cells, affirming their epithelial lineage despite their mesenchymal morphology. Co-expression of vimentin is very common and reflects the mesenchymal differentiation. Other markers can be informative: TTF-1 is typically negative in SpCC (more common in adenocarcinomas). Markers of squamous differentiation, like p63 or p40, are also usually negative, unless there is an admixed squamous cell carcinoma component (classifying it as a pleomorphic carcinoma). Exclusionary markers for true sarcomas (desmin for leiomyosarcoma, S100 for MPNST or melanoma, SOX10 for melanoma) are crucial in the differential diagnosis, especially when cytokeratin expression is weak or focal. The presence of spindle cells can also be found in tumors of the mediastinum, kidney, thyroid, and breast.[19,20]

The patient's presentation with profound neurological deficits and imaging evidence of extensive local destruction vividly illustrates the aggressive infiltrative capacity of SpCC. This is not merely a passive expansion but an active process of tissue degradation and invasion. The destruction of the VTh4 vertebra is a stark testament to the tumor's osteolytic capabilities. Malignant SpCC cells, endowed with enhanced motility and invasiveness through EMT, can directly infiltrate bone tissue. They achieve this by secreting a cocktail of proteolytic enzymes, particularly matrix metalloproteinases (MMPs such as MMP-2, MMP-9) and cathepsins. These enzymes degrade the components of the bone's extracellular matrix (collagen, proteoglycans), literally carving a path for the invading tumor cells. Tumor cells are master manipulators of the bone microenvironment. They secrete factors (such as parathyroid hormone-related protein (PTHrP), interleukin-6 (IL-6), tumor necrosis factor-alpha (TNF-α), and prostaglandins) that

stimulate the differentiation and activity of osteoclasts—the primary bone-resorbing cells. A key pathway involved is the RANK/RANKL/OPG system. Tumor cells can express RANKL (Receptor Activator of Nuclear factor Kappa-B Ligand), which binds to its receptor RANK on osteoclast precursors and mature osteoclasts, promoting their activation and survival. This leads to excessive bone resorption. As the bone matrix is degraded, growth factors sequestered within it (such as TGF-β, insulin-like growth factors (IGFs)) are released, which can further stimulate tumor cell proliferation, creating a "vicious cycle" of bone destruction and tumor growth. While direct extension from the paravertebral mass is the most likely route of vertebral invasion in this case, Batson's venous plexus offers an alternative. This valveless network of veins runs longitudinally along the vertebral column and communicates freely with segmental veins from the thorax, abdomen, and pelvis. Tumor emboli can travel through this plexus, bypassing systemic circulation, to seed the vertebral bodies. The rich sinusoidal network within vertebral marrow provides a fertile ground for tumor cell arrest and proliferation. Lung tumors can invade the spinal canal via Batson's plexus or directly through arteries to the vertebral corpus. The patient's lower limb weakness, spasticity, hyperreflexia, and Babinski signs are classical indicators of an upper motor neuron lesion, specifically affecting the corticospinal tracts. The erosion of VTh4 and likely epidural extension of the tumor would cause direct compression of the spinal cord at this thoracic level. The diminished sensation below T8-T10 suggests involvement of the spinothalamic tracts. Spinal cord compression can lead to direct mechanical injury to axons and neurons, as well as ischemic damage due to compromised blood supply (to the anterior spinal artery or radicular arteries). Edema and inflammatory responses further exacerbate the neural dysfunction. The relatively rapid progression of symptoms over four months is consistent with the aggressive growth rate of SpCC. Invasion of the spinal canal is frequently caused by mediastinal masses, though it can also be found with lung masses. The 0.5 cm compression and displacement of the descending aorta highlight the sheer bulk and infiltrative pressure exerted by the SpCC. Large thoracic tumors, especially those situated in the confined space of the posterior mediastinum, can displace, encase, or compress major vascular structures. While SpCC is not typically known for vascular invasion to the extent of, for example, angiosarcomas, its sheer bulk and infiltrative nature can lead to significant compression. Such compression can potentially compromise blood flow, although clinical sequelae depend on the degree and chronicity of the compression and the presence of collateral circulation. The robust contrast enhancement seen within the tumor on CT signifies a hypervascular nature, a common feature in many aggressive malignancies, including SpCC, driven by tumor-induced angiogenesis. This vascularity supports rapid growth but also provides routes for hematogenous dissemination. The effacement of the fat plane between the mass and the aorta on CT is a concerning sign, suggesting close adherence or micro-invasion. A lung tumor may first invade the mediastinal pleura, narrow the descending aorta, and then infiltrate the spinal canal.

The radiological presentation of this SpCC as a posterior mediastinal mass is what makes this case particularly instructive. Less than 5% of pulmonary SpCCs adopt this disguise. However, specific imaging features, when carefully analyzed, hinted at its true pulmonary origin. The observation that the mass formed an acute angle with the mediastinal pleura is a key indicator. This sign is based on the principle of growth dynamics. A mass originating within the lung parenchyma, as it expands and pushes against the mediastinum, tends to mold itself into the pleural space, creating a sharp, acute interface. Conversely, a primary mediastinal mass expanding outwards often displaces the lung, creating a smoother, obtuse angle with the pleural surface. The underlying pathophysiology relates to differential tissue resistance and the direction of growth vectors. The irregular interface between the mass and the adjacent

lung parenchyma on CT is a direct visual correlate of the infiltrative growth pattern of malignant cells into the surrounding normal lung tissue. Malignant cells do not typically expand as a smooth, pushing front but rather send out microscopic projections and individual cells into the surrounding tissue, resulting in an ill-defined or spiculated border. Lobulation of the tumor contour often reflects uneven or multifocal growth within the mass, possibly due to varying rates of proliferation in different tumor segments or the coalescence of initially separate tumor foci. Locating the geometric center (epicenter) of the tumor can provide clues to its site of origin. In this case, although the tumor occupied a significant portion of the posterior mediastinum, its epicenter appeared to be at the lung-mediastinal junction, favoring origin from the peripheral lung with secondary extension into the mediastinum. A tumor originating deep within mediastinal structures would likely have its epicenter clearly within the mediastinum, with secondary compression or invasion of the lung. The avid and relatively uniform contrast enhancement of the mass signifies a highly vascular tumor. As discussed, SpCC, like many aggressive malignancies, induces robust angiogenesis to support its metabolic demands and rapid growth. The contrast medium, an iodinated solution, fills these neovessels, leading to increased attenuation on CT. The "isodense" appearance on pre-contrast images suggests a solid, cellular tumor without large areas of cystic change or macroscopic necrosis (though microscopic necrosis is common in SpCC). The degree of enhancement can correlate with tumor grade and aggressiveness. The foci of peripheral calcification seen in this tumor are most likely dystrophic. Dystrophic calcification occurs in areas of chronic inflammation, necrosis, or hemorrhage within a tumor. As tumor cells die, particularly in rapidly growing lesions that may outstrip their blood supply in certain areas, the necrotic tissue can undergo calcification. While not specific to SpCC, its presence in such an aggressive mass is consistent with these processes. Speculation on factors that might lead to this unusual growth pattern (such as specific site of origin near the hilum/mediastinal pleura, particular genetic drivers influencing infiltrative patterns) is warranted. The inherent plasticity afforded by EMT might allow certain SpCC clones to more readily adapt to growth within the mediastinal environment, exploiting fascial planes or paths of least resistance differently than conventional NSCLCs.

When confronted with an aggressive posterior mediastinal mass causing vertebral erosion, several entities are typically considered, each with its own pathophysiological basis. These arise from Schwann cells, perineurial cells, or fibroblasts of the peripheral nerve sheaths. Their posterior mediastinal location is common due to the presence of intercostal nerves and the sympathetic chain. MPNSTs, the malignant variant, are highly aggressive sarcomas known for local invasion, including bone erosion and foraminal extension (producing "dumbbell tumors"). Cytologically, they are spindle cell tumors, necessitating IHC for differentiation (S100, SOX10 positivity). Various other sarcoma types (such as fibrosarcoma, leiomyosarcoma) can arise in the mediastinum. These are mesenchymal malignancies characterized by infiltrative growth and potential for bone destruction. Cytologically, they are spindle cell neoplasms, and differentiation from SpCC relies heavily on demonstrating epithelial markers in SpCC and specific mesenchymal lineage markers in sarcomas. While some lymphomas (such as diffuse large B-cell lymphoma) can be aggressive and cause bone erosion, their cytomorphology is typically round blue cells, distinct from spindle cells. They often present with bulky lymphadenopathy, which was not a dominant feature here apart from the primary mass itself. Given the patient's history of breast cancer, a metastasis to the posterior mediastinum/vertebra was an initial concern. Breast cancer, particularly lobular carcinoma, can metastasize to unusual sites. Metaplastic carcinoma of the breast, a rare subtype, can contain spindle cell components and behave aggressively. However, the FNA morphology, if strongly suggestive of a primary lung sarcomatoid process, coupled with a typical SpCC immunoprofile (if

obtained), would argue against this. Metastases reach bone via hematogenous spread, often establishing in the marrow and then causing osteolysis through similar mechanisms (osteoclast activation) as primary tumors.

The diagnosis of SpCC in this patient was ultimately a synthesis of seemingly disparate clues. The insidious onset of progressive myelopathy pointed to a growing lesion impinging on the spinal cord. The history of breast cancer initially raised the possibility of metastasis, but the de novo presentation of a large, aggressive thoracic mass with distinct imaging characteristics on CT—particularly the acute angle sign and irregular lung interface —began to steer suspicion towards a primary thoracic malignancy, potentially of pulmonary origin despite its mediastinal dominance. The FNA cytology, revealing malignant spindle cells within a fibroangiomatous stroma, was pivotal. This morphology, while not exclusive to SpCC, is highly characteristic, especially in the context of a lung-associated mass. The aggressive features (vertebral erosion, aortic compression) over a relatively short symptomatic period of four months are entirely congruent with the known aggressive biology of SpCC, driven by its underlying EMT and genetic alterations. The tumor's ability to erode bone and compress major vessels speaks to its unbridled growth and production of factors that mediate tissue destruction and invasion. This case profoundly illustrates that SpCC is not merely a pathological curiosity but a clinically aggressive entity whose behavior is a direct consequence of its complex cellular and molecular alterations. Its capacity to mimic other conditions, such as a primary mediastinal tumor, necessitates a high index of suspicion and a meticulous, multidisciplinary approach to diagnosis, integrating clinical acumen, sophisticated imaging interpretation, and expert pathological analysis. The aggressive nature and poor prognosis associated with spindle cell carcinoma make accurate diagnosis crucial for planning appropriate management.

4. Conclusion

This case report describes a rare and diagnostically challenging presentation of pulmonary spindle cell carcinoma (SpCC) in a 47-year-old woman, where the tumor radiologically mimicked an aggressive primary posterior mediastinal mass with associated vertebral erosion and aortic compression. Despite the initial appearance, meticulous evaluation of the chest X-ray and, more definitively, the contrast-enhanced CT scan revealed subtle but crucial signs suggestive of a pulmonary origin. These included the acute angle formed by the mass with the mediastinum, an epicenter appearing to be based at the lung-mediastinal interface with growth into the lung, and the irregular nature of the tumor-lung boundary. The CT-guided Fine Needle Aspiration cytology was instrumental in establishing the diagnosis of SpCC, revealing characteristic atypical polymorphic spindle cells. This case underscores that while SpCC typically presents as a peripheral lung mass, it can, in rare instances, manifest as a predominantly mediastinal lesion, thereby creating a significant diagnostic dilemma with true mediastinal tumors. The aggressive local invasion observed, including destruction of the thoracic vertebra and compression of the descending aorta, is consistent with the known aggressive biology of SpCC. Although spinal canal invasion is often associated with posterior mediastinal neurogenic tumors, this case demonstrates that aggressive primary lung cancers can also present with similar patterns of invasion. The diagnosis of SpCC carries a generally poor prognosis, and management is often multimodal, involving consideration of surgery, chemotherapy, radiotherapy, and increasingly, targeted therapies or immunotherapy based on molecular profiling. The central (suprahiler) location in this instance suggested squamous cell carcinoma as a potential underlying epithelial component, influencing histopathological considerations. Ultimately, this report highlights the critical importance of integrating detailed clinical information, advanced multimodal imaging findings, and expert cytopathological analysis in arriving at an accurate diagnosis for rare and

atypically presenting thoracic malignancies. A high index of suspicion for uncommon variants of lung cancer is necessary when faced with aggressive thoracic masses, even those appearing to arise from the mediastinum. Effective interdisciplinary collaboration is paramount in navigating these complex cases to ensure optimal patient management and to contribute to a better understanding of these rare oncological entities.

5. References

1. Naso J, Desai A, Smith CJ, Ashara YP, Yip S, Lo Y-C. Predictive value and molecular correlates of MYC immunohistochemistry and copy number gain in non-small cell lung carcinomas treated with immunotherapy. Lung Cancer. 2024; 195(107927): 107927.
2. Zhang T, Goel A, Xu X, Wu Y, Tang E, Zhang F, et al. N-mytistoyltransferase 1 and 2 are potential tumor suppressors and novel targets of miR-182 in human non-small cell lung carcinomas. Lung Cancer. 2022; 171: 70–81.
3. Adachi H, Ito H, Isaka T, Murakami K, Miura J, Kikunishi N, et al. Effect of surgical treatment for N2-positive c-stage III non-small cell lung carcinoma in the "PACIFIC" era. Clin Lung Cancer. 2023; 24(8): 733–42.
4. Yuan T, Ni P, Zhang Z, Wu D, Sun G, Zhang H, et al. Targeting BET proteins inhibited the growth of non-small cell lung carcinoma through downregulation of Met expression. Cell Biol Int. 2023; 47(3): 622–33.
5. Park C-K, Oh I-J, Kim Y-C. Role of adjuvant treatment in stage IB non-small cell lung carcinoma. Transl Lung Cancer Res. 2023; 12(3): 649–52.
6. Park C-K, Oh I-J, Kim Y-C. Role of adjuvant treatment in stage IB non-small cell lung carcinoma. Transl Lung Cancer Res. 2023; 12(3): 649–52.
7. Nishimatsu K, Matsumoto Y, Kashima J, Imabayashi T, Uchimura K, Furuse H, et al. Concordance between cryobiopsy and forceps biopsy specimens in assessment of immunohistochemistry staining for non-small cell lung carcinoma. Transl Lung Cancer Res. 2023; 12(6): 1245–55.
8. Kim JW, Kim M-J, Han T-H, Lee J-Y, Kim S, Kim H, et al. FSP1 confers ferroptosis resistance in KEAP1 mutant non-small cell lung carcinoma in NRF2-dependent and -independent manner. Cell Death Dis. 2023; 14(8): 567.
9. Fang F, Zhao M, Jin X, Dong Z, Wang J, Meng J, et al. RETRACTED ARTICLE: Upregulation of MCL-1 by LUCAT1 through interacting with SRSF1 promotes the migration and invasion in non-small cell lung carcinoma. Mol Cell Biochem. 2023.
10. Aoki M, Miyata R, Kamimura G, Morizono S, Tokunaga T, Harada-Takeda A, et al. Successful long-term outcome of neoadjuvant sequential targeted therapy and chemotherapy for stage III non-small cell lung carcinoma: 10 case series. Transl Lung Cancer Res. 2024; 13(12): 3278–88.
11. Ding X, Li X, Jiang Y, Li Y, Li H, Shang L, et al. RGS20 promotes non-small cell lung carcinoma proliferation via autophagy activation and inhibition of the PKA-Hippo signaling pathway. Cancer Cell Int. 2024; 24(1): 93.
12. Demir Cevizlidere B, Uysal O, Avci H, Gunes Bagis S, Semerci Sevimli T, Dincer M, et al. Establishment, culture and characterization of gemcitabine hydrochloride-resistant human non-small cell lung carcinoma cell line derived cancer stem cells. Cell Biochem Funct. 2024; 42(4).
13. Parra-Medina R, Castañeda-González JP, Montoya L, Gómez-Gómez MP, Clavijo Cabezas D, Plazas Vargas M. PD-L1 expression in non-small cell lung carcinoma in Latin America: a systematic review and meta-analysis. Transl Lung Cancer Res. 2024; 13(7): 1660–71.

14. Wasik A, Podhorska-Okolow M, Dziegiel P, Piotrowska A, Kulus MJ, Kmiecik A, et al. Correlation between periostin expression and pro-angiogenic factors in non-small-cell lung carcinoma. Cells. 2024; 13(17): 1406.
15. Fayyaz A, Basit M, Farooq A, Khan T, Ayub U, Khan S, et al. Therapeutic potential of ethoxy mansonone G: a comprehensive exploration of its anticancer actions in breast cancer, colorectal cancer, and non-small cell lung carcinoma. Cell Biol Int. 2024; 48(9): 1229–39.
16. Uprety D, Roden AC, Peters S. Adjuvant immunotherapy should be used in patients with non-small cell carcinoma with a pathologic complete response to neoadjuvant immunotherapy. J Thorac Oncol. 2025; 20(1): 34–8.
17. Zhao Y, Dhani S, Gogvadze V, Zhivotovsky B. The crosstalk between SND1 and PDCD4 is associated with chemoresistance of non-small cell lung carcinoma cells. Cell Death Discov. 2025; 11(1): 34.
18. Ahn B, Kim D, Ji W, Chun S-M, Lee G, Jang SJ, et al. Clinicopathologic and genomic analyses of SMARCA4-mutated non-small cell lung carcinoma implicate the needs for tailored treatment strategies. Lung Cancer. 2025; 201(108445): 108445.
19. Ceccarelli S, Pasqua Marzolesi V, Vannucci J, Bellezza G, Floridi C, Nocentini G, et al. Toll-like receptor 4 and 8 are overexpressed in lung biopsies of human non-small cell lung carcinoma. Lung. 2025; 203(1): 38.
20. Liu N, Li X, Luo X, Liu B, Tang J, Xiao F, et al. Development and validation of machine learning models based on molecular features for estimating the probability of multiple primary lung carcinoma versus intrapulmonary metastasis in patients presenting multiple non-small cell lung cancers. Transl Lung Cancer Res. 2025; 14(4): 1118–37.